IEEE Photonics Journal
An IEEE Photonics Society Publication

Open Access

# Fiber Supercontinuum Source for Broadband-CARS Microspectroscopy Based on a Dissipative Soliton Laser

Volume 9, Number 4, August 2017

**Yan Li**
**Xiaosheng Xiao, *Member, IEEE***
**Lingjie Kong**
**Changxi Yang**

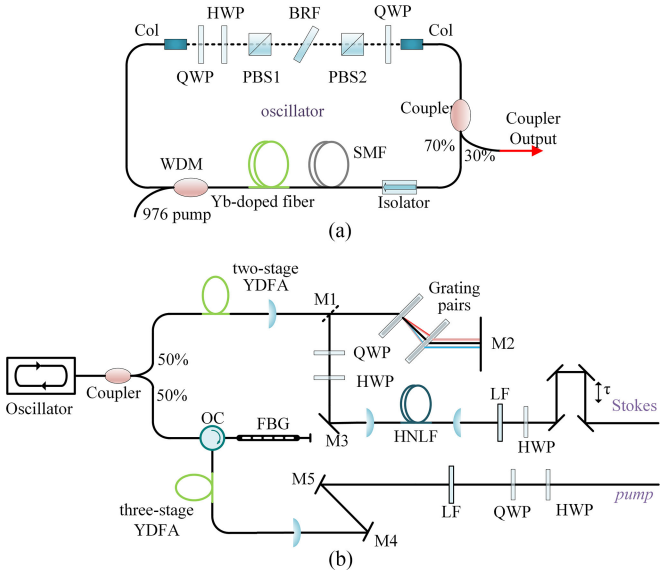


DOI: 10.1109/JPHOT.2017.2712648
1943-0655 © 2017 IEEE

IEEE photonics SOCIETY

IEEE

# Fiber Supercontinuum Source for Broadband-CARS Microspectroscopy Based on a Dissipative Soliton Laser

**Yan Li, Xiaosheng Xiao, *Member, IEEE*, Lingjie Kong, and Changxi Yang**

State Key Laboratory of Precision Measurement Technology and Instruments, Department of Precision Instruments, Tsinghua University, Beijing 100084, China

*DOI:10.1109/JPHOT.2017.2712648*


Manuscript received April 4, 2017; revised May 30, 2017; accepted June 2, 2017. Date of publication June 8, 2017; date of current version June 23, 2017. This work was supported in part by the National Natural Science Foundation of China under Grant NSFC 51527901, in part by the National Program for Significant Scientific Instruments Development of China under Grant 2011YQ030134, and in part by the Initiative Research Program of State Key Laboratory of Precision Measurement Technology and Instruments. Corresponding author: Xiaosheng Xiao (e-mail: xsxiao@tsinghua.edu.cn.)

**Abstract:** We propose and demonstrate a supercontinuum fiber laser source for broadband coherent anti-Stokes Raman scattering (BCARS) microspectroscopy, seeded by a Yb-doped dissipative soliton fiber laser. Smooth continuum Stokes pulses ranging from 1050 to 1312 nm at –20 dB bandwidth are generated in a highly nonlinear fiber from the compact fiber seed, and the corresponding pump pulses are obtained after a narrowband filter centered at 1036 nm. With this fiber laser source, we are able to obtain BCARS spectra in 700–1900 $cm^{-1}$ spectral range simultaneously with resolution less than 10 $cm^{-1}$, and show its application in analyzing complex mixture. We also demonstrate the capability of our system in chemical imaging by simultaneously obtaining two two-dimensional CARS images of retinoic acid crystal at Raman shifts of ∼1574 and ∼1162 $cm^{-1}$, respectively.

**Index Terms:** Fiber lasers, non-linear microscopy, supercontinuum generation, Raman spectroscopy.

## 1. Introduction

Coherent anti-Stokes Raman scattering (CARS) microscopy is a sensitive, chemical selective, label-free imaging technique, which has found broad applications in chemistry, biology and medicine [1], [2]. CARS is a kind of four-wave mixing (FWM) [3]. When the light fields of *pump* ($\omega_p$) and Stokes ($\omega_s$) interact with the sample, if the frequency difference of the *pump* and Stokes lasers matches the Raman-active vibrational frequency ($\omega_v$) of a molecule (i.e. $\omega_p - \omega_s = \omega_v$), the resonance-enhanced anti-Stokes signal ($\omega_{CARS}$) can be generated [2], [3]. Typical laser sources for CARS microscopy are generally expensive and complex, which utilize solid-state lasers to generate synchronized pulses to act as *pump* and Stokes beams, even though the parameters provided by these systems are suitable for the CARS process [4]–[7]. Fiber lasers that can potentially meet those features for CARS, have the advantages in good beam quality, compact structure, and low cost, which makes CARS microscopy promising for chemical analysis and practical clinic applications [8]–[15].

Compared to spontaneous Raman microscopy, CARS microscopy is a promising and an alternative approach to obtain vibrational spectroscopic images at high acquisition speeds [16]. CARS

microscopy includes narrowband CARS microscopy and broadband CARS (BCARS, or multiplex CARS) microspectroscopy. Narrowband CARS microscopy features rapid imaging acquisition by working at a fixed Raman shift, which, however, makes it difficult to analyze complex samples [17]. In contrast, BCARS microspectroscopy can identify the complete spectral band of the complex sample simultaneously for quantitative analysis [18]. So far, BCARS has been widely employed in various spectroscopic applications with moderate acquisition time [8], [16], [18].

For BCARS, a broadband Stokes laser ($\omega_s$) and a narrowband *pump* laser ($\omega_p$) are required, so that multiple vibrational modes ($\omega_v$) can be achieved simultaneously. In [19]–[21], BCARS microspectroscopy was demonstrated by virtue of picosecond *pump* (probe) and wavelength-tunable femtosecond Stokes. These approaches had high spectral resolution while the spectral bandwidth was not sufficient in diagnosing complex samples. Other techniques employed supercontinuum (SC) Stokes, generated in highly nonlinear fibers, to achieve BCARS microspectroscopy [22]–[25]. SC-based BCARS microspectroscopy can cover a broadband vibrational spectrum simultaneously, which shows promise in biochemical analysis and imaging.

The SC is used as the Stokes beam, which is the key element in a SC-based BCARS system. Both solid-state lasers [22], [23] and fiber lasers [24] have been employed to generate SC in those BCARS systems. In [24], the seed, a stretched-pulse fiber laser, firstly decreased the repetition rate to 0.5 MHz in order to obtain high energy pulse and avoid the nonlinear phase noise in the amplification, then filtered to narrowband pulses with 106 ps duration, eventually the SC Stokes pulses were generated by degenerate FWM in a photonic crystal fiber (PCF) pumped by the narrowband pulses. Another scheme of ultrafast-pulse laser, dissipative soliton fiber laser (or ANDi fiber laser) [14], [26], [27], has attracted lots of attentions recently. It has a simple structure without dispersion-compensation components inside the laser cavity, and gives a high output pulse-energy. As a seed of chirped pulse amplification, dissipative soliton fiber laser can be amplified by all-fiber structure without stretcher, and be compressed to femtosecond pulse, which is convenient for SC generation.

In this paper, we demonstrate a fiber laser source for BCARS microspectroscopy, based on a Yb-doped dissipative soliton fiber laser. The SC Stokes pulses are generated from the compact seed, and the corresponding *pump* pulses are obtained by a narrowband fiber Bragg grating (FBG). We achieve CARS signal with spectral range of $700-1900\,\mathrm{cm}^{-1}$ simultaneously, and demonstrate the capability of our fiber SC source for BCARS system in analyzing the mixture of polystyrene and retinoic acid, as an example. We also demonstrate the capability of our system in biochemical imaging, by obtaining three-dimensional CARS images ($x$-$y$-$\lambda$) of retinoic acid crystal.

## 2. Experimental Setup

The setup of fiber source for BCARS microspectroscopy is shown in Fig.1. A Yb-doped dissipative soliton oscillator served as the seed laser (Fig. 1(a)), which is similar to our former report [28]. The seed was mode-locked by nonlinear polarization rotation (NPR), and a 30:70 fiber coupler was inserted after the free-space component. We chose the 30% output from the fiber coupler port as the seed, since we have found that the SC originated from the coupler port is broader than that from the NPR port [28]. The average output power, spectral bandwidth and center wavelength of the seed are 11.6 mW, 12 nm and 1036 nm (Fig. 2(a)), respectively. It delivered a 30 MHz, 5.2 ps (FWHM, Fig. 2(b)) pulse train with a time-bandwidth product of 17.44.

The output pulses were split into two beams using a 50:50 fiber coupler. One beam was first amplified by a two-stage all-fiber Yb-doped fiber amplifier (YDFA) to 500 mW. No pre-chirp before amplification is necessarily due to the inherent advantage of dissipative soliton laser in highly chirped output. Then it was compressed by a pair of gratings, followed by being coupled into a highly nonlinear PCF for SC generation. A 0.6 m PCF with zero dispersion wavelength of 1035 nm was used for SC generation. After a 1050 nm long-pass filter, we achieved Stokes beam spanning from 1050 to 1312 nm at $-20$ dB bandwidth (black curve in Fig. 2(c)).

The other beam was first filtered by a FBG, and then amplified with a three-stage all-fiber YDFA. The output pulses, with average power up to 500 mW, were used as the *pump* beam. In order to

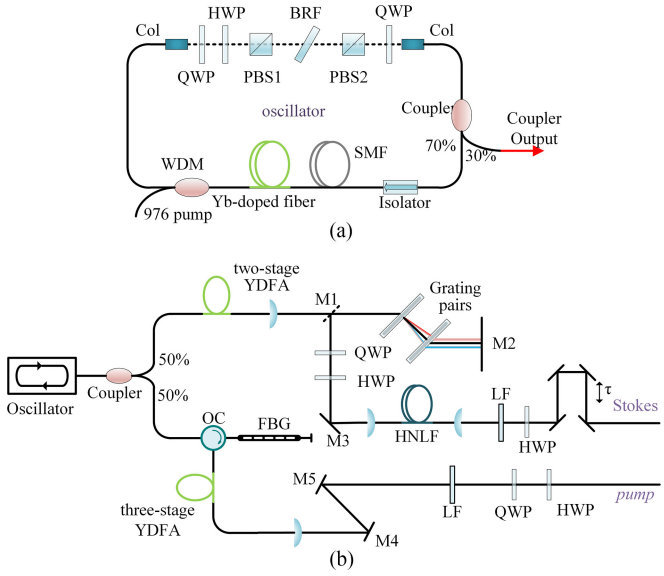


Fig. 1. Diagram of the source for BCARS microspectroscopy. (a) Yb-doped dissipative soliton fiber oscillator. (b) Fiber SC source for BCARS microspectroscopy. Col: collimator; WDM: wavelength division multiplexer; SMF: single-mode fiber; HWP: half wave plate; QWP: quarter wave plate; PBS: polarization beam splitter; BRF: birefringent plate; YDFA: Yb-doped fiber amplifier; OC: optical circulator; FBG: fiber Bragg grating; M: mirror; HNLF: highly-nonlinear fiber; LF: long-pass filter.

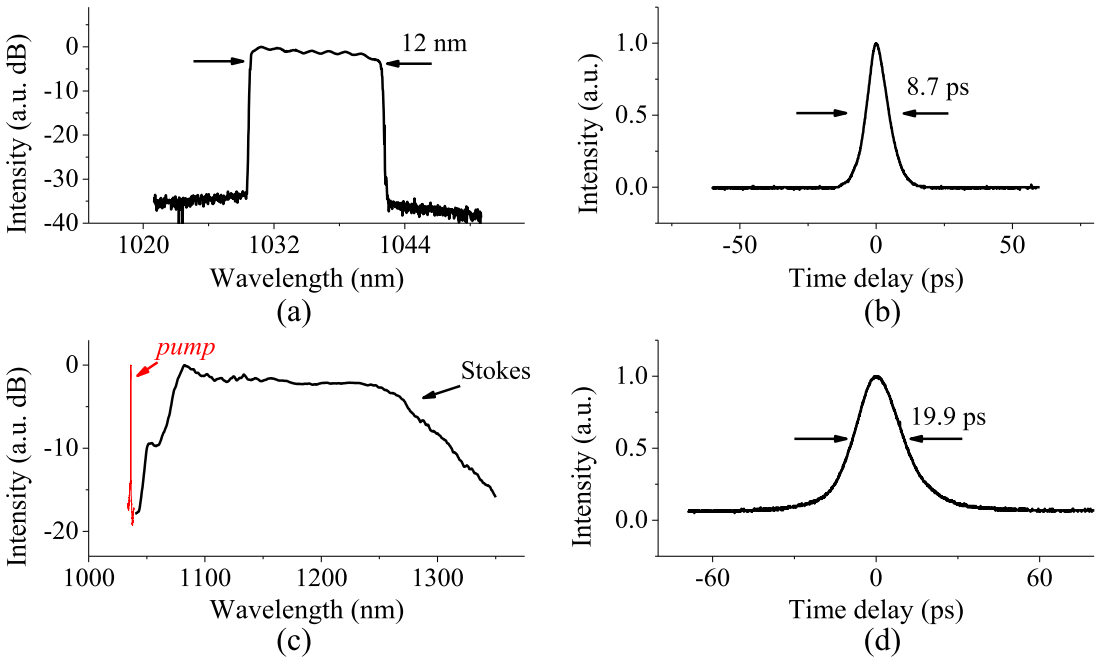


Fig. 2. Output characteristics of the fiber SC source for BCARS microspectroscopy. (a) Optical spectrum of the seed. (b) Autocorrelation trace of the seed. (c) Spectra of Stokes beam (black, input average power of highly-nonlinear fiber is 325 mW) and *pump* beam (red, bandwidth of 0.23 nm). (d) Autocorrelation trace of *pump* beam.

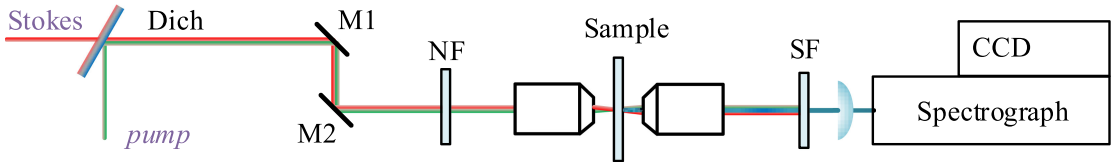


Fig. 3. Schematic of experimental setup for BCARS microspectroscopy with the fiber SC source. Dich: dichroic mirror; M: mirror; NF: notch filter; SF: short-pass filter.

obtain a narrowband *pump* beam, two different FBGs were tried with bandwidths of 0.1 nm and 0.25 nm, centered at 1036.25 nm and 1036.14 nm, respectively. Both these two *pump* beams met the high resolution ($<10\,\mathrm{cm}^{-1}$) feature for CARS process. Eventually the latter FBG (0.25 nm bandwidth) was adopted in our system to ensure higher peak power due to the shorter pulse duration. The bandwidth and pulse durations of the amplified *pump* pulses were 0.23 nm (red curve in Fig. 2(c), measured with spectral resolution of 0.06 nm) and 11.9 ps (Fig. 2(d)), respectively, which indicates that the pulses were slightly chirped with a time-bandwidth product of 0.765. A 1000 nm long-pass filter was placed in *pump* beam to reject the residual 976 nm pump. A tunable delay stage in the Stokes beam was used to adjust the temporal overlap of *pump* and Stokes beams. Quarter wave plates and half wave plates were used to adjust the polarization states of both beams. The overall pump power for the fiber source was about 6 W.

We then employed the proposed fiber SC source in BCARS microspectroscopy (Fig. 3). The *pump* and Stokes beams were combined by a 1064 nm dichroic mirror. Two microscope objectives were used subsequently, to focus the excitation beams (numerical aperture 0.42) and to collect the forward CARS signal (numerical aperture 0.29), respectively. In order to further reject the residual 976 nm pump, a 980 nm notch filter was placed before the focusing objective. The CARS signal passed through a 1000 nm short-pass filter and was detected by a spectrograph (HORIBA IHR320) attached with a front-illuminated CCD (HORIBA Synapse 1024 $\times$ 256).

## 3. Results and Discussion

To demonstrate the performance of our source in BCARS microspectroscopy, we acquired the CARS spectra of polystyrene, retinoic acid (Sigma R2625) and the mixture of these two over the $700-1900\,\mathrm{cm}^{-1}$ spectral range (Fig. 4).

The samples were placed on a precision manual stage (*x-y-z*) with 0.5 $\mu$m accuracy. *Pump* and Stokes powers at the sample were 140 mW and 8.4 mW, respectively. A CARS signal at the Raman shifts ($\sim$1002 $\mathrm{cm}^{-1}$, $\sim$1031 $\mathrm{cm}^{-1}$, $\sim$1155 $\mathrm{cm}^{-1}$, $\sim$1180 $\mathrm{cm}^{-1}$, $\sim$1579 $\mathrm{cm}^{-1}$ and $\sim$1600 $\mathrm{cm}^{-1}$) of polystyrene (black curve in Fig. 4(a)) and the Raman shifts ($\sim$1012 $\mathrm{cm}^{-1}$, $\sim$1162 $\mathrm{cm}^{-1}$ and $\sim$1574 $\mathrm{cm}^{-1}$) of retinoic acid (black curve in Fig. 4(b)) were observed within the fingerprint region. The corresponding Raman spectra (red curve in Fig. 4(a) and (b)) were measured with a home-made (spontaneous) Raman microspectroscopy system excited by a 785 nm laser (Thorlabs FPL785S-250). For the mixtures, the BCARS spectra of polystyrene and retinoic acid could be obtained simultaneously (Fig. 4(c)), which suggested the capability of our system in distinguishing and quantifying chemical mixtures. There is an offset between the broadband CARS and Raman spectra due to the presence of non-resonance background in CARS, which making the raw CARS spectra shifted toward the lower frequencies with respect to the spontaneous Raman spectra. Numerical algorithms (e.g. Kramers-Kronig phase retrieval [18]) could be employed to retrieve the true Raman spectrum.

The CARS images (*x-y-*$\lambda$) of an irregular retinoic acid crystal (inset of Fig. 5) were obtained by a preliminary imaging experiment with field of view 114 $\times$ 82 $\mu\mathrm{m}^2$ (57 $\times$ 41 pixels). The imaging process was obtained by moving the sample stage in *x-y* plane every 2 $\mu$m, with the laser spot being focused on a *z*-plane of the sample. For imaging, two microscope objectives were replaced to focus the excitation beams (numerical aperture 0.75, Olympus XLPLN25XWMP2 used in the

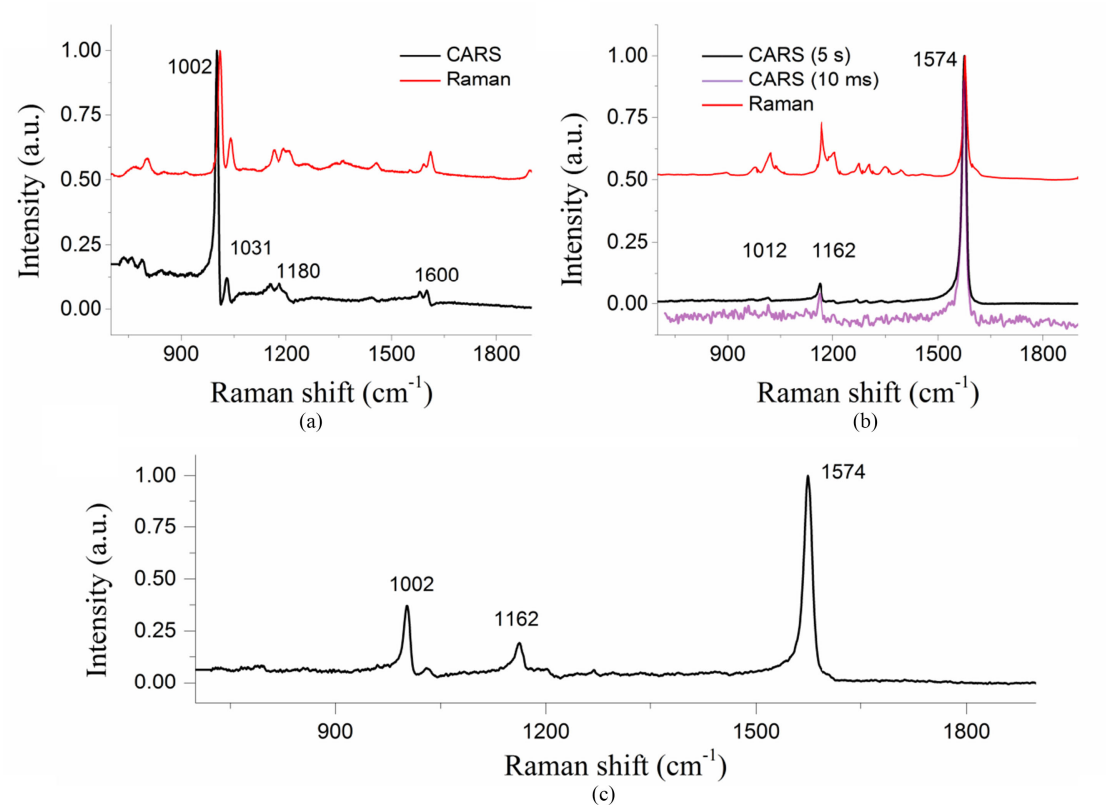


Fig. 4. CARS spectrum measured with the proposed fiber SC source. (a) Spontaneous Raman (red) and CARS (black) spectra of polystyrene (b) Spontaneous Raman and CARS spectra of retinoic acid. (c) CARS spectra of the mixture. For the purpose of comparing the complete spectra including the weak peaks, the acquisition time of both CARS and Raman spectra are 5 seconds. A CARS spectrum with 10 ms acquisition time is also given in (b).

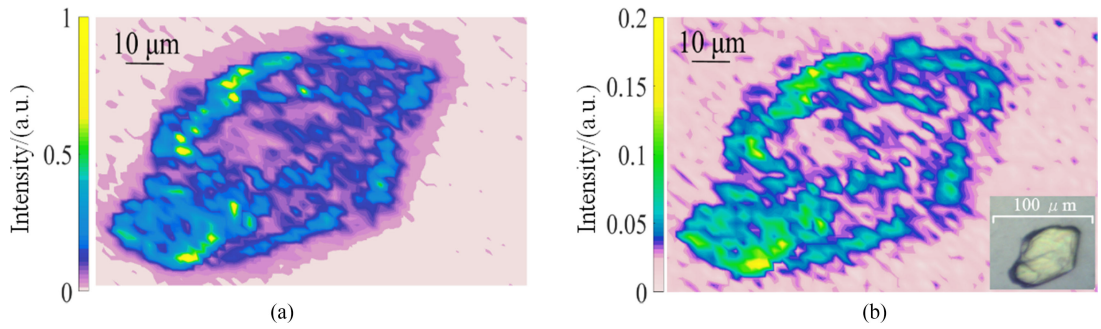


Fig. 5. The CARS image ($x$-$y$-$\lambda$) of an irregular retinoic acid crystal (inset: CCD imaging of the sample) at Raman shifts of (a) ~1574 $cm^{-1}$ and (b) ~1162 $cm^{-1}$.

air) and to collect the forward CARS signal (numerical aperture 0.42), respectively. From Fig. 5, the images at Raman shifts ~1574 $cm^{-1}$ (Fig. 5(a)) and ~1162 $cm^{-1}$ (Fig. 5(b)) were well-matched, which showed the capability of our system in chemical imaging.

In current experiment, a full BCARS spectrum at a single pixel could be obtained in tens of milliseconds scale, which was mainly limited by the low efficiency of Stokes focusing (28%) and CARS signal collection (36%). For the future work, the speed could be enhanced by optimizing the

microscopy, i.e. the optical components after the beams combining. Besides, to further improve the capabilities of the BCARS-source in bioimaging, frequency conversion can be used to convert the 1036 nm *pump* pulses to around 800 nm, which could increase the spectral bandwidth of the CARS spectrum to access lipid region.

## 4. Conclusion

We demonstrated a BCARS microspectroscopy based on a SC fiber source, seeded by a dissipative soliton fiber laser. The Yb-doped mode-locked oscillator delivered a 30 MHz, 5.2 ps (FWHM) pulse train with large chirp. The narrowband *pump* pulses (0.23 nm centered at 1036.14 nm) and smooth SC Stokes pulses ranging from 1050 to 1312 nm at $-20$ dB bandwidth were generated from the compact fiber laser. To demonstrate the performance of our source in BCARS microspectroscopy, we obtained the CARS spectra of polystyrene, retinoic acid and the mixture of these two over the $700-1900\,\mathrm{cm}^{-1}$ spectral range simultaneously with high resolution ($<10\,\mathrm{cm}^{-1}$). We also demonstrated the CARS image ($x$-$y$-$\lambda$) of retinoic acid at Raman shifts of $\sim$1574 $\mathrm{cm}^{-1}$ and $\sim$1162 $\mathrm{cm}^{-1}$ simultaneously. The results suggest the capability of our system in distinguishing and quantifying chemical mixtures, promising in biochemical imaging.

## References


[1] C. H. Camp, Jr., and M. T. Cicerone, "Chemically sensitive bioimaging with coherent Raman scattering," *Nature Photon.*, vol. 9, no. 5, pp. 295–305, Apr. 2015.

[2] J. Cheng and X. S. Xie, "Vibrational spectroscopic imaging of living systems: An emerging platform for biology and medicine," *Science*, vol. 350, no. 6264, Nov. 2015, Art. no. aaa8870.

[3] M. D. Levenson, *Introduction to Nonlinear Laser Spectroscopy*, London, U.K.: Academic, 1982.

[4] H. Kano and H. Hamaguchi, "In-vivo multi-nonlinear optical imaging of a living cell using a supercontinuum light source generated from a photonic crystal fiber," *Opt. Exp.*, vol. 14, no. 7, pp. 2798–2804, Apr. 2006.

[5] F. Ganikhanov, S. Carrasco, X. Sunney Xie, M. Katz, W. Seitz, and D. Kopf, "Broadly tunable dual-wavelength light source for coherent anti-Stokes Raman scattering microscopy," *Opt. Lett.*, vol. 31, no. 9, pp. 1292–1294, May 2006.

[6] B. Chen, J. Sung, and S. Lim, "Chemical imaging with frequency modulation coherent anti-Stokes Raman scattering microscopy at the vibrational fingerprint region," *J. Phys. Chem. B*, vol. 114, no. 50, pp. 16871–16880, Dec. 2010.

[7] R. Mouras, P. O. Bagnaninchi, A. R. Downes, and A. P. D. Elfick, "Label-free assessment of adipose-derived stem cell differentiation using coherent anti-Stokes Raman scattering and multiphoton microscopy," *J. Biomed. Opt.*, vol. 17, no. 11, Nov. 2012, Art. no. 116011.

[8] C. H. Camp *et al.*, "High-speed coherent Raman fingerprint imaging of biological tissues," *Nature Photon.*, vol. 8, no. 145, pp. 627–634, Aug. 2014.

[9] M. Marangoni, A. Gambetta, C. Manzoni, V. Kumar, R. Ramponi, and G. Cerullo, "Fiber-format CARS spectroscopy by spectral compression of femtosecond pulses from a single laser oscillator," *Opt. Lett.*, vol. 34, no. 21, pp. 3262–3264, Nov. 2009.

[10] S. Lefrancois *et al.*, "Fiber four-wave mixing source for coherent anti-Stokes Raman scattering microscopy," *Opt. Lett.*, vol. 37, no. 10, pp. 1652–1654, May 2012.

[11] E. S. Lamb, S. Lefrancois, M. Ji, W. J. Wadsworth, X. S. Xie, and F. W. Wise, "Fiber optical parametric oscillator for coherent anti-Stokes Raman scattering microscopy," *Opt. Lett.*, vol. 38, no. 20, pp. 4154–4157, Oct. 2013.

[12] M. Baumgartl *et al.*, "All-fiber laser source for CARS microscopy based on fiber optical parametric frequency conversion," *Opt. Exp.*, vol. 20, no. 4, pp. 4484–4492, Feb. 2012.

[13] M. Chemnitz *et al.*, "Widely tuneable fiber optical parametric amplifier for coherent anti-Stokes Raman scattering microscopy," *Opt. Exp.*, vol. 20, no. 24, pp. 26583–26595, Nov. 2012.

[14] E. S. Lamb and F. W. Wise, "Multimodal fiber source for nonlinear microscopy based on a dissipative soliton laser," *Biomed. Opt. Exp.*, vol. 6, no. 9, pp. 3248–3255, Aug. 2015.

[15] K. Chen, T. Wu, H. Wei, T. Zhou, and Y. Li, "Dual-soliton Stokes-based background-free coherent anti-Stokes Raman scattering spectroscopy and microscopy," *Opt. Lett.*, vol. 41, no. 11, pp. 2628–2631, Jun. 2016.

[16] C. M. Hartshorn *et al.*, "Multicomponent chemical imaging of pharmaceutical solid dosage forms with broadband CARS microscopy," *Analytical Chem.*, vol. 85, pp. 8102–8111, Jul. 2013.

[17] C. L. Evans, E. O. Potma, M. Puoris'haag, D. Côté, C. P. Lin, and X. S. Xie, "Chemical imaging of tissue in vivo with video-rate coherent anti-Stokes Raman scattering microscopy," *Proc. Nat. Acad. Sci.*, vol. 102, no. 46, pp. 16807–16812, Nov. 2005.

[18] Y. J. Lee, D. Moon, K. B. Migler, and M. T. Cicerone, "Quantitative image analysis of broadband CARS hyperspectral images of polymer blends," *Analytical Chem.*, vol. 83, pp. 2733–2739, Mar. 2011.

[19] H. A. Rinia, K. N. J. Burger, and M. Muller, "Quantitative labelfree imaging of lipid composition and packing of individual cellular lipid droplets using multiplex CARS microscopy," *Biophys. J.*, vol. 95, no. 10, pp. 4908–4914, Nov. 2008.

[20] M. Bonn, M. Muller, and K. N. J. Burger, "Imaging of chemical and physical state of individual cellular lipid droplets using multiplex CARS microscopy," *J. Raman Spectrosc.*, vol. 40, no. 7, pp. 763–769, Jul. 2009.

[21] E. R. Andresen, C. K. Nielsen, J. Thogersen, and S. R. Keiding, "Fiber laser-based light source for coherent anti-stokes Raman scattering microspectroscopy," *Opt. Exp.*, vol. 15, no. 8, pp. 4848–4856, Apr. 2007.
[22] T. W. Kee and M. T. Cicerone, "Simple approach to one-laser, broadband coherent anti-Stokes Raman scattering microscopy," *Opt. Lett.*, vol. 29, no. 23, pp. 2701–2703, Dec. 2004.
[23] H. Kano and H. Hamaguchi, "Ultrabroadband ($>$2500 cm$^{-1}$) multiplex coherent anti-Stokes Raman scattering microspectroscopy using a supercontinuum generated from a photonic crystal fiber," *Appl. Phys. Lett.*, vol. 86, no. 12, Mar. 2005, Art. no. 121113.
[24] T. Gottschall *et al.*, "Fiber-based source for multiplex-CARS microscopy based on degenerate four-wave mixing," *Opt. Exp.*, vol. 20, no. 11, pp. 12004–12013, May 2012.
[25] S. Michel, A. Courjaud, E. Mottay, C. Finot, J. Dudley, and H. Rigneault, "Polarized multiplex coherent anti-Stokes Raman scatting using a picosecond laser and a fiber supercontinuum," *J. Bio. Opt.*, vol. 16, no. 2, pp. 11081–11084, Feb. 2011.
[26] A. Chong, J. Buckley, W. Renninger, and F. Wise, "All-normal-dispersion femtosecond fiber laser," *Opt. Exp.*, vol. 14, no. 21, pp. 10095–10100, Oct. 2006.
[27] X. Xiao, Y. Hua, B. Fu, and C. Yang, "Experimental investigation of the wavelength tunability in all-normal-dispersion ytterbium-doped mode-locked fiber lasers," *IEEE Photon. J.*, vol. 5, no. 6, Dec. 2013, Art. no. 1502807.
[28] X. Xiao and Y. Hua, "Supercontinuum generation based on all-normal-dispersion Yb-doped fiber laser mode-locked by nonlinear polarization rotation: Influence of seed's output port," *Opt. Commun.*, vol. 377, pp. 94–99, Oct. 2016.